ELSEVIER

Journal of Non-Crystalline Solids 194 (1996) 191–197

JOURNAL OF NON-CRYSTALLINE SOLIDS

New thermally induced color centers in lithium borate tungstate glasses, $(Li_2B_4O_7)_{100-x}(WO_3)_x$

M. Wollenhaupt [a], H. Ahrens [a], P. Fröbel [a], K. Bärner [a], E.R. Giessinger [b], R. Braunstein [b,*]

[a] *4. Physikalisches Institut, Universität Göttingen, Bunsenstr. 11–15, D-37073 Göttingen, Germany*
[b] *University of California, Los Angeles, Physics Department, Hilgard Ave., Los Angeles, CA 90095, USA*

Received 21 September 1994; revised 5 June 1995

Abstract

A new color center based on a local structural and chemical change of the average borate tungstate glass matrix has been identified. The matrices of the colored glasses all had a 1:1 ratio of $Li_2B_4O_7$ and WO_3 except for glasses with $x = 0$. The reaction took place in air and at 1200 K in all cases, while the reaction time varied between 10 and 60 min. Subsequent to reaction, the glasses were cooled to 550 K in 1 min and then annealed in air at that temperature for 2 h. The coloration starts at a critical temperature $T_c = 630$ K and needs latent sites. The coloration process involves a distribution of energy barriers for the migration of Li^+ with half-width comparable to its mean value, 2.91 eV. The achieved center concentrations are estimated to lie between 0.3 and 3 mol%. In addition, a color center has been found which is connected with Fe^{+3} impurities. This coloration is reversible and connected with a temperature-induced shift, 5×10^{-4} eV/K, of the Fe-based oscillators.

1. Introduction

Colored glasses can generally be divided into two classes according to whether the generation of color centers is reversible or irreversible. Both classes have specific applications, the most prominent being the reversible darkening of sunglasses [1,2] and the (irreversible) coloring of utility glasses [3,4]. Lithium borate tungstate glasses also have a color center of both types: a reversible photochromic blue coloration has been observed in the presence of hydrogen and was later attributed to the formation of tungsten bronzes H_xWO_3 [4,5]. Thermally activated generation of a permanent blue color has also been observed [6]; that center ('B') has been related to lithium tungsten bronzes, Li_xWO_3 [7]. The reversible coloration has been proposed for use in displays [5,15,16]. Fig. 1 shows the characteristic absorption connected with two new thermally activated color centers; one center ('Y') is obtained through Fe-doping, is reversible on heating and cooling and leads to a yellowish tinge by comparison with the undoped transparent glass. Originally, the Fe-doping was introduced to furnish a standard colored glass, to be

* Corresponding author. Tel: +1-310 825 1841. Telefax: +1-310 206 5668. E-mail: braunstein@physics.ucla.edu.

SSDI 0022-3093(95)00460-2

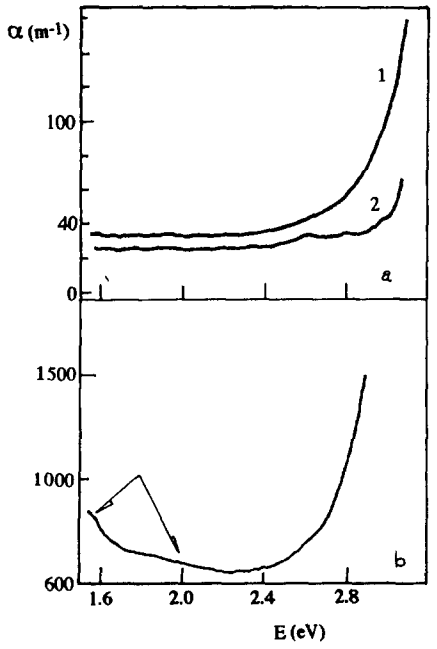

Fig. 1. Absorption constant versus quantum energy, $\alpha(E)$, for the G- (irreversible) and Y- (reversible) color centers. (a) Y, 3 mol% Fe: 1, 300 K; 2, 650 K. (b) G (arrows: possible W^{+5} related absorption bands).

used for comparison, but no single Fe-specific absorption peak with height proportional to the Fe content was observed in the visible spectral region. However, later its thermally induced coloration and its spectral similarity with the other color center was discovered, again justifying its use as a standard. A second center ('G') is irreversible, based on a local structural modification and leads to a greenish tinge by comparison with the center-free transparent glass. For that, in particular, thermal treatments can be applied which would allow the manufacture of a series of green glasses with transparency between 90 and 5%. Aside from their potential applications, the borate–tungstate glasses appear to be useful model systems for the understanding of reversible and irreversible coloring processes in glasses.

2. Preparational

As the generation of the structurally based permanent B- and G-type color centers depends somewhat on the WO_3 starting material used, we have specified this source more precisely: W(IV)O_3 (Riedel de Haen, 99.5%/Lot #14310, loss on ignition 0.1%; 0.01%: Mo,SO_4; 0.005%: Ca, Cl; 0.001%: Fe, Pb). The sources of the dopant Fe (Alpha products) and of the borate $Li_2B_4O_7$ (Riedel de Haen, 99%; 0.005%: Ca, Na, Cl, SO_4; 0.002%: K, Mg, Pb, PO_4: 0.0005% Fe) are not critical. We also used a constant sample mass (4 g) and reaction temperature (1200 K), as both the reaction temperature and the cooling time have an influence on the coloration [8]. This effect is also produced by the reaction time, t_r, which was varied between 10 and 60 min (see Fig. 3(b), Table 1). After the reaction, the liquid was poured (1 min) into hollow forms which were kept at

Table 1
Composition, reaction time, dielectric constant and color of some of the glass samples (reaction temperature 1200 K)

$Li_2B_4O_7$ (mol%)	WO_3 (mol%)	Reaction time (min)	Dielectric constant	Final color	Remarks
100	0	30		transparent	
50	50	22	10.0	transparent	
50	50	22	11.1	greenish	thermal color 1
50	50	22	13.0	green	thermal color 2
50	50	22	15.1	grey/green	recrystallized
50	50	10	15.1	deep blue	
50	50	12	14.0	deep blue	
50	50	15	12.1	blue	
50	50	20	11.0	blue	
99.8	0	40		transp./yellow	0.2 mol% Fe
			3.7		quartz glass

a temperature of 550 K. Subsequently, the samples were annealed at that temperature for 2 h. The glass transition temperature is ~ 690 K for $x = 0.5$ samples [6].

Depending on use, different geometrical shapes were made. Table 1 shows some preparation properties and the final color of the dielectric constant of some of the glasses which were investigated. The sample faces were polished using SiC paper (grain sizes: 220/360/600/1000) in connection with a plane grinding equipment (Struers, DP10) and finely polished using diamond paste (Winter-diplast, grin sizes: 7/3/1 μm). The X-ray diffractions of the glasses ($0 \leq x \leq 0.5$) had no Bragg reflections up to their recrystallization temperature, T_r.

3. Experimental

A temperature controlled oven was construction to allow the measurement of the optical transmission at elevated temperatures (300 K < T < 800 K) [9]. The sample temperature was usually measured using a thermocouple tip which was inserted into a cylindrical hole drilled into the sample. The oven was positioned in front of the entrance slit of the monochromator of a conventional spectrometer which is described elsewhere [8]. The spectrometer was tested using a standardized Schott glass (BG-20); its resolution was ≈ 2 Å. For some of the coloration experiments, only a monochromatic beam (Spectra 124 A, 15 mW, $\lambda = 6328$ Å) had to be directed through the sample (inside the oven) and detected by a PIN diode (RCA C30808). If a temperature cycle, $T(t)$, was applied, it was recorded simultaneously with the transmitted intensity, $I(t)$. To spectrally resolve measurements, $I(\lambda)$ was generally normalized by dividing by the intensity with the sample taken out, $I_0(\lambda)$, thus giving the transmission, τ, as

$$\tau = I/I_0 = \exp(-\alpha x); \quad (1)$$

at the same time, τ was standardized to a sample thickness of 1 mm. The dielectric constant was measured on glass disks with two evaporated gold electrodes and using conventional equipment (Philips RLC meter PM 6303). The reference reflectivity of the samples did not vary much with the color: it was close to 8%; see also Ref. [8].

4. Results

4.1. Thermally induced coloration

Fig. 2(a) shows an example of a coloration produced by a thermal treatment $T(t)$ in non-Fe-doped 1:1 borotungstate samples; note that up to 630 K no

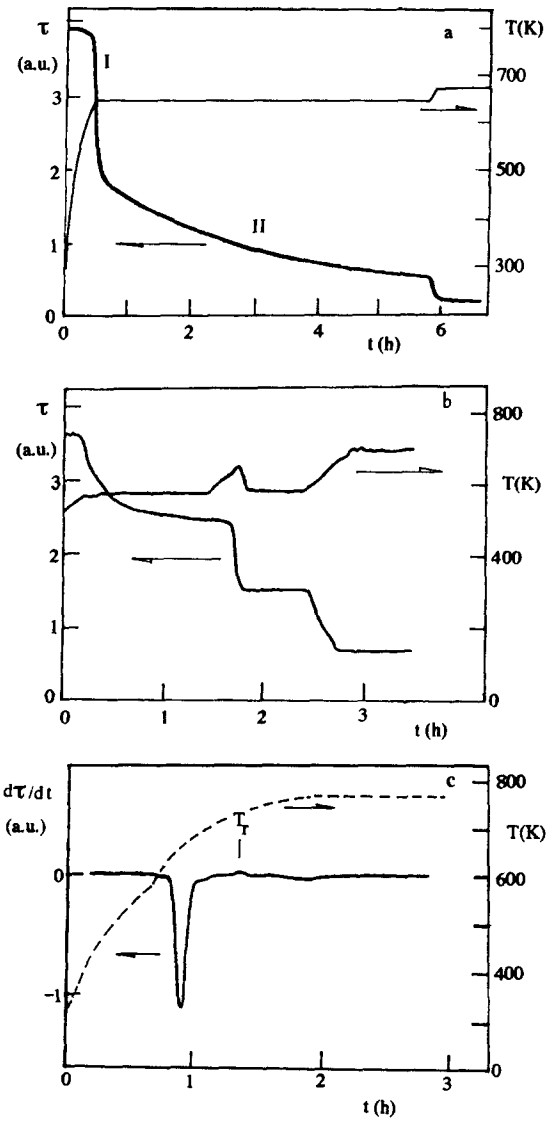

Fig. 2. (a) Transmitted intensity versus time, $\tau(t)$, and heating curve, $T(t)$, for a thermally G-colored $x = 50$ sample. $\lambda = 6328$ Å. Halting temperature: $T_1 = 650$ K. (b) Stepwise coloration achieved by incremental changes $\pm \Delta T_1$ of the halting temperature T_1. $\lambda = 6328$ Å. (c) Differential transmitted intensity $d\tau/dt$, together with $T(t)$, showing the onset of coloration and recrystallization ($T_r = 730$ K). $\lambda = 6328$ Å.

coloration was observed; this temperature is labeled T_f. When a temperature $T_1 > T_f$ was reached, the main coloration (I) appeared while the temperature T_1 was unchanged.

One observes a second, slower, coloration regime (II). The time for this coloration was decreased by elevating the temperature $T_1 \rightarrow T_1 + \Delta T$. Fig. 2(b) shows that it was possible to stop the changing transmission at any time by reducing the temperature, $T_1 \rightarrow T_1 - \Delta T$, while Fig. 2(c) shows that the coloration precedes the recrystallization. $d\tau/dt$ shows a small structure close to the recrystallization temperature, T_r, as given by Ref. [6]. We also find that no further coloration occurs at temperature $> T_r$.

4.2. Critical coloration temperature

The increase of the coloration in a rather narrow temperature interval whose lower boundary defines

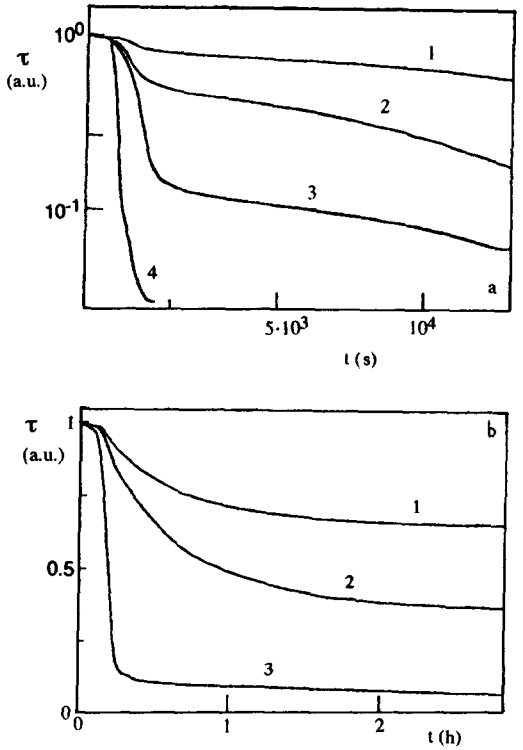

Fig. 3. (a) Coloration curves $\tau(t)$ for different temperatures close to the critical coloration temperature, T_f. 1,2,3,4: T_1 = 630 K, 650 K, 660 K, 680 K, respectively. t_r = 22 min; λ = 6328 Å. (b) Coloration curves obtained for the same halting temperature, T_1 = 660 K, but using different reaction times, t_r, of the melt. λ = 6328 Å. 1,2,3: t_r = 60 min, 40 min, 22 min.

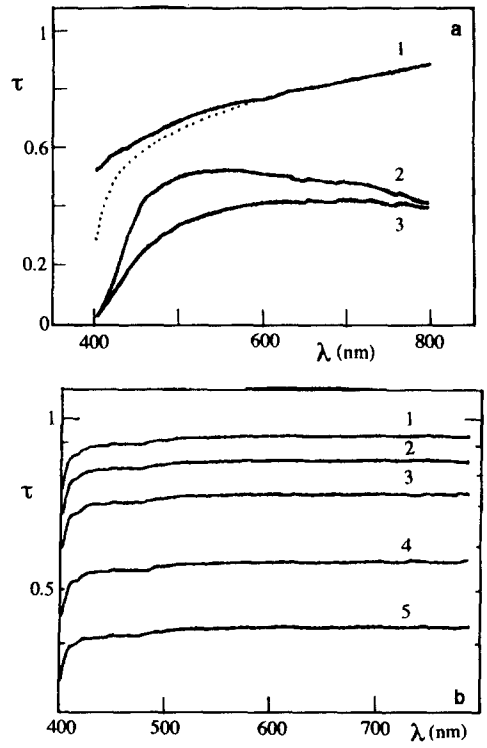

Fig. 4. (a) Decrease of the transmission, τ, of a x = 50 glass after a two-step thermal coloration (G-center): 4000 Å < λ < 8000 Å. 1: heated without coloration. T_1 = 500 K, 2 h; dashed line: T_1 = 600 K, 2 h. 2: coloration after the first stage: T_1 = 650 K, 2 h. 3: coloration after the second stage: T_1 = 650 K, 2 h. (b) Spectral distribution of the transmission, $\tau(\lambda)$, for different $(Li_2B_4O_7)_{100-c}Fe_c$ glasses. 1,2,3,4,5 = 0.2, 0.5, 1, 2, 3 at.% Fe. 4000 Å < λ < 8000 Å.

the critical coloration temperature, T_f, can be shown also by measuring $\tau(t)$ at small increments of a temperature T_1 which is kept constant for each measurement (Fig. 3(a)). Again, the $\tau(t)$ curves cannot be fitted to a single exponential time constant or generation rate. Also, different $\tau(t)$ curves are obtained using the same T_1s and reaction temperatures, T_m, but different reaction times, t_r (Fig. 3(b)). A similar dependence on reaction time has been found also for the B-type color center [8].

4.3. Spectral distribution of the coloration

Fig. 4(a) shows the reduction in transmission versus wavelength as produced by the G-center. A slight temperature effect is already observed for the spectrum of the G-center free transparent glass (dashed line). Aside from this, the thermally induced

coloration produces a spectral distribution similar to the Fe-doping (Fig. 4(b)), which suggests a similar cause (a color center). In particular, a charge transfer band of Fe^{+3} is expected to occur around 350 nm [1,7].

Fig. 4(b) shows the Fe-induced transmission for different dopant contents, c, at room temperature. We do not have a single sharp absorption band which increased in height with c while the baseline remained constant, but rather a 'grey' spectra, one which increased in height with c at all measured wavelengths. For the G-center, the spectrum changed from the first (curve 2) to the second (curve 3) annealing stage; this change cannot be explained by an increase in the number of G-centers alone.

5. Discussion

5.1. Number densities

When we write the time-dependent intensity, $I(\lambda,t)$, as

$$I(t) = I_0 \exp(-\beta(t)t) \quad \text{and} \quad \beta(t) = (1/\tau)\mathrm{d}\tau/\mathrm{d}t, \tag{2}$$

the extraction of $\beta(t)$ from the data (time constant spectroscopy) is indicated. This extraction has been done (Fig. 5), and shows one rather well defined peak which corresponds to the coloration regime I. As for a purely exponential increase of the number density of color centers, the generation rate, g, would be proportional to β, as $g = \mathrm{d}t/\mathrm{d}t = \beta N$; equivalently to Eq. (2), we write

$$N_c \sim \int \beta(t)\,\mathrm{d}t \tag{3}$$

and, from Fig. 5, by integration (as indicated for $t_r = 22$ min, $T_1 = 660$ K, $T_m = 1200$ K) we obtain the ratio (8:1) between the G-type color centers produced in the first and second coloration stages; the oscillator strengths, f_i [10], are assumed to be the same. From Eq. (3), absolute values of N_c cannot be obtained. We can, however, estimate the absolute number densities in two ways. If we assume comparable oscillator strengths for the Y- (Fe-based) and the G-center, we obtain $N_c \approx 2.8$ mol%. The second possibility is to convert the number densities of the B-color center, $N_c = 10^{19}$ to 10^{20} cm^{-3} from Ref. [11]. Then, we obtain 0.25–2.5 mol%.

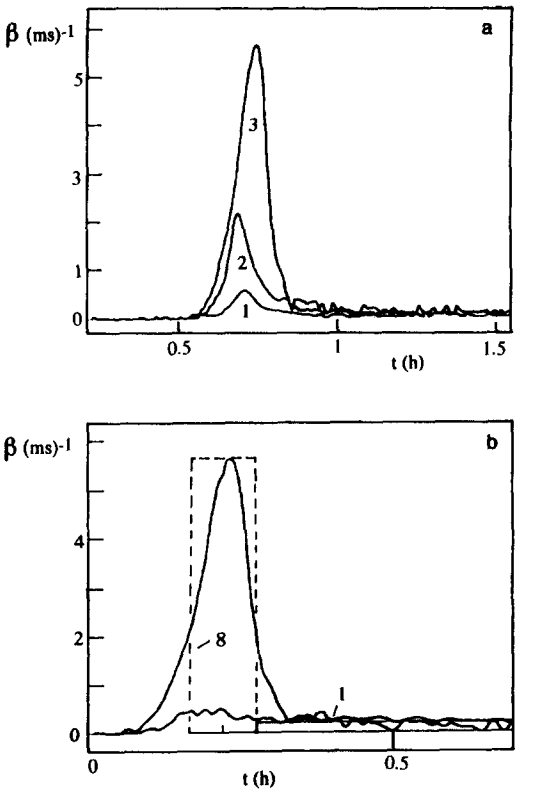

Fig. 5. (a) Slightly time-dependent time constant, $\beta(t)$, as extracted from Figs. 3(a) and (b) using Eq. (2): 1,2,3: $T_1 = 630$ K, 650 K, 660 K: $\lambda = 6328$ Å. (b) $\beta(t)$ for two different reaction times. Upper curve: $t_r = 22$ min; lower curve: $t_r = 40$ min: $T_1 = 660$ K, $\lambda = 6328$Å. Boxes: approximate peak integration; the area ratio is 8:1. For more details, see text.

5.2. Coloration processes

5.2.1. Fe-based color center ('Y')

Accidental Fe-doping has been observed in the electron spin resonance (ESR) spectra of these glasses [7] and Fe^{+3} in an orthorhombic symmetry has been identified [12]. With the doping used here, the Lambert–Beer law is observed (Fig. 4(b)), i.e., Fe is sufficiently diluted to rule out changes of the glass matrix [13]. From Fig. 4(b), we suggest an overlap of many Fe-based oscillators, whose density or oscillator strengths increase towards the short wavelength end of the spectrum and then merge with the fundamental absorption of the glass matrix. The reversible coloration (Fig. 1(b)) can then be attributed to a temperature-induced shift of some or all of the Fe-based oscillators to higher wavelengths. Such shifts

are generally relation to anharmonic effects [13], i.e., $\Delta E_m \approx (20\ \text{eV}\ \text{Å}^2) 2 b_1 T / a_0^2$ (b_1 is the linear expansion coefficient; a_0 is the average bond length for $T > 0$) [13,14]. For $\Delta T = 350$ K, $a_0 = 4$ Å, $b_1 = 10^{-4}$, we obtain $\Delta E_m \approx 0.08$ eV and with it 2×10^{-4} eV/K; indeed a value close to the experimentally observed shift (Fig. 1(b)). For the non-doped borate glass the absorption edge also shifts with the temperature but the edge is at a higher energy, 3.3 eV(300 K), and this does not lead to a coloration in the visible [6].

5.2.2. B-type color center

Reversible blue coloration has been observed in thin WO_3 films and has been assigned to intervalence charge transfer according to the photoreaction [15]

$$W^{+5}(A) + W^{+6}(B) + hf \leftrightarrow W^{+6}(A) + W^{+5}(B)$$

but only in the presence of injected protons, H^+ which reduces a W^{+6} to W^{+5} (tungsten bronze) [16]. For the permanently blue colored glasses, the same bronze process has been claimed [7] although with a broader distribution of the B-center configurations and involving Li^+ ions. As this coloration functions only at elevated temperatures, we suggest that a thermally activated transport of the Li^+ ions [9,21] is a prerequisite:

$$n_{Li} = n_0 \exp(-\langle E_0 \rangle / kT), \tag{4}$$

where n_{Li} is the activated fraction per energy interval, n_0 is the available Li per energy interval and $\langle E_0 \rangle$ is the distribution of activation energy barriers. As the Li^+ carrier densities are estimated to be 10^{19} in the coloration regime [17], for the initial coloration (stage I) the transport of the Li^+ ions is expected to be the coloration rate limiting process; at a later state (II), however, a limitation by the number of available latent sites, which in this context appear as deep traps for the Li^+ ions, is likely.

5.2.3. G-type color center

5.2.3.1. Configuration of the G-center. A greenish coloration has been observed earlier with Cu-doped lithium borotungstate glasses but could not be assigned to the Cu^{+2} color centers which give a blue borate glass. Instead, the simultaneous presence of W^{+5} had to be assumed, but notably only for $x > 20$ at.% WO_3 [18]. Consistently, ESR measurements identified ionic W^{+5} signals for $x > 20$ at.% which decayed when the B-type coloration set in Ref. [7]; apparently the charge transfer state competes with a W^{+5} crystal field state. For this W^{+5}, state a C_{4v} point group symmetry [19] and oscillators at 1.4 and 2.2 eV [20] were proposed; the optical spectrum of the G-center (Fig. 1, arrows) indeed has two shallow peaks, one < 1.6 eV and the other ≈ 2.0 eV, aside from the rise at 2.8 eV which has to be assigned to the fundamental absorption.

5.2.3.2. Latent sites. The reduction of the coloration with increasing time (Fig. 3(b)) indicates latent sites for the G-color centers which are performed already in the liquid which are finally destroyed if one uses long reaction times. A similar dependence on reaction time has been found for the B-centers [8] and has been interpreted in terms of $(WO_3)_n$ clusters which were supposed to constitute the latent sites, i.e., the deep Li^+ traps [7]. For the G-centers, however, the reduction of W^{+6} with the trapping of a Li^+ in such a cluster would have to occur without a charge transfer state.

5.2.3.3. Coloration process. In principle, for the G-coloration process, the arguments used with the B-center should be valid (see Section 5.2.2.). However, the coloration connected with the G-center has been investigated more systematically. The $\tau(t)$ curves can be described by two distributions of time constants (see Fig. 5). From that maximal, time constants could be extracted for both regimes and these are compiled in Table 2; β_{max} is almost constant for regime II, while it is exponentially rising for regime I, i.e.,

$$\beta_{max}^{I} = \beta_0 \exp(-E_C / kT). \tag{5}$$

Table 2
Time constants, β, of the coloration process

Coloration temperature T_1 (K)	Slow coloration (II) β_1 (10^{-5} s^{-1})	Fast coloration (I) β_2 (10^{-3} s^{-1})	Calculated (Eq. (5))
626	2.7	0.5	0.45
646	7.4	2.2	2.50
656	6.4	5.6	5.73
675	7.8	25.6	25.6

From Table 2 and Eq. (5) we find: $\beta_0 = 8.1 \times 10^{20}$ s^{-1} while $E_C = 2.91$ eV; clearly, this activation energy is of the size of the binding energy, which varies between 3.5 and 2.9 eV depending on the WO_3 content [6]. As both the migration of Li^+ through vacant sites or interstitial positions of the glass network might have activation energies of this order of magnitude, we cannot decide on the particular Li^+ transport mechanism here. A δ-distribution of the barrier activation energy at $E = E_c$, however, would not suffice to explain the rise in coloration at T_f. Therefore, we have to assume a (exponentially rising) barrier distribution $\langle E_0 \rangle$; only if this distribution becomes activated from the low energy end could we hope to obtain a sufficiently steep coloration onset. We can estimate the width of the activation energy barrier distribution as follows: integration of Eq. (4) using a rectangular barrier function $(E_0, \Delta E_0)$ gives the total activated Li, N_{Li}; the total amount of color centers, N_c, is obtained from Eq. (3) using another rectangular barrier function $\beta_{max}, \Delta t_0)$; then setting $N_{Li} = N_c$, we find $E_0 \approx E_C$. As the low energy end of the barrier distribution, $E_0 - \Delta E_0/2$, should coincide with the onset of the coloration, i.e., $kT_f = 0.05$ eV, we would have the halfwidth of the activation energy barrier distribution in the same order of magnitude as the mean value.

6. Conclusions

Three different types of coloration have been found in tungstate borate glasses. One of them is reversible and related to the Fe-doping (Y-center). The two other colorations are irreversible (B- and G-type centers). As the creation of the G-centers is similar to that of the B-center which in turn is close to a tungsten bronze defect H_xWO_3, we assume specific clusters $(WO_3)_m$ and a local Li^+ induced reduction of W^{+6} but instead of charge transfer states, we observe a distribution of W^{+5} crystal field states. In both cases the latent sites become active only through thermally activated transport of Li^+. We conclude that the barrier activation energies have a broad distribution which makes it possible to observe a coloration well below the melting and recrystallization temperatures.

Acknowledgements

The authors thank the Deutsche Forschungsgemeinschaft for partial support. This work was also supported by the Universitywide Energy Research Group of the University of California and the National Renewable Energy Laboratory.

References

[1] N.J. Araujo and N.F. Borelli, Optical Properties of Glass (Academic Press, Orlando, FL, 1990) p. 320.
[2] D.M. Trotter and D.W. Smith, Appl. Phys. Lett. 45 (1984) 112.
[3] S.D. Stookey, G.H. Beall and J.E. Pierson, J. Appl. Phys. 49 (1978) 5114.
[4] D.R. Uhlmann and N.J. Kreidl, Uhlmann, Glass Forming Systems, Vol. 1 (Academic Press, New York, 1983) p. 160.
[5] R. Braunstein, Solid State Commun. 28 (1978) 843.
[6] Ch. Ruf, K. Bärner and R. Braunstein, Solid State Commun. 54 (1985) 111.
[7] M.v. Dirke, S. Müller, K. Bärner and H. Rager, J. Non-Cryst. Solids 124 (1990) 265.
[8] P. Fröbel and K. Bärner, J. Non-Cryst. Solids 88 (1986) 329.
[9] M. Wollenhaupt, diploma thesis, Universität Göttingen (1992).
[10] Y.R. Zakis, A.R. Lusis and Y.L. Lagzdons, J. Non-Cryst. Solids 47 (1982) 267.
[11] J. Trost, P. Fröbel and K. Bärner, Solid State Commun. 81 (1992) 201.
[12] E. Guedes de Sousa, S.K. Mendiratta and J.M. Machado da Silva, Portugal Phys. 17 (1986) 203.
[13] W.A. Weyl, Colored Glasses (Charlesworth, Sheffield, 1951) p. 103.
[14] K.H. Hellwege, Einführung in die Festköperphysik (Springer, Berlin, 1988) p. 55.
[15] B.W. Faughan and R.S. Crandall, Appl. Phys. 40 (1980) 181.
[16] O.F. Schirmer, V. Wittwer, G. Baur and G. Brandt, J. Electrochem. Soc./Solid State 124 (1977) 749.
[17] M. Sayer and G.F. Lynch, J. Phys. C6 (1973) 3675.
[18] R. Staske, P. Fröbel and K. Bärner, J. Lumin. 55 (1993) 115.
[19] A. Goldstein, V. Chiriac and D. Becherescu, J. Non-Cryst. Solids 92 (1987) 271.
[20] F. Studer, N. Rih and B. Raveau, J. Non-Cryst. Solids 107 (1988) 101.
[21] D. Deal, M. Burd and R. Braunstein, J. Non-Cryst. Solids 52 (1985) 111.